



Regular Article

Evaluation of single crystal elastic constants and stacking fault energy in high-nitrogen duplex stainless steel by *in-situ* neutron diffraction



Yanghoo Kim^a, Yong Min Kim^a, Ji-Yeon Koh^a, Tae-Ho Lee^b, Wan Chuck Woo^c, Heung Nam Han^{a,*}

^a Department of Materials Science and Engineering and Research Institute of Advanced Materials, Seoul National University, Seoul 151-744, Republic of Korea

^b Ferrous Alloy Department, Korea Institute of Materials Science, 531 Changwondaero, Changwon 641-831, Republic of Korea

^c Neutron Science Division, Korea Atomic Energy Research Institute, Daejeon 305-353, Republic of Korea

ARTICLE INFO

Article history:

Received 22 January 2016

Received in revised form 14 March 2016

Accepted 15 March 2016

Available online 1 April 2016

Keywords:

Stainless steels

Neutron diffraction

Nanoindentation

Stacking fault energy

ABSTRACT

Single crystal elastic constants of austenite and ferrite phases in high-nitrogen duplex stainless steel were evaluated by an elastic self-consistent model combined with an optimization process using *in-situ* neutron diffraction data. The optimized elastic constants were validated by the indentation moduli of each phase obtained by nanoindentation. In addition, the stacking fault energy of austenite was evaluated based on the neutron diffraction profile and the single crystal elastic constants and was subsequently correlated with the observed deformation microstructure.

© 2016 Elsevier Ltd. All rights reserved.

Duplex stainless steels (DSSs), which offer several outstanding features, such as high strength and good corrosion resistance relative to other single austenitic grades, have attracted interest for many years [1,2]. To reduce costs, nitrogen-added DSSs were recently found to achieve a reduction in Ni and to offer improvements in both the strength and corrosion resistance [3]. However, due to the different mechanical properties of its constituent phases, austenite (γ) and ferrite (α) in DSS, inhomogeneous deformation is inevitable [3–10]. This drawback makes it difficult to predict the overall mechanical behavior of DSS, and it necessitates the appropriate characterization of the mechanical properties of each phase. To observe the mechanical behavior of each phase in DSS, *in-situ* neutron diffraction (ND), which can access the lattice strain development of individual phases during the deformation process, has been shown to be a useful tool [7–11].

In an effort to understand the inhomogeneous deformation behavior of high-nitrogen DSS, the present work aims to evaluate the mechanical properties including the single crystal elastic constants of each phase and the stacking fault energy (SFE) of γ , and to discuss the deformation behavior of nitrogen-strengthened γ in DSS in terms of the SFE. First, the evolution of several lattice strains during tensile deformation was measured by *in-situ* ND. The single crystal elastic constants of each phase were optimized by an elastic self-consistent (ESC) model with the lattice strain data and the information of the phase and grain orientation measured by electron back scattered diffraction (EBSD). The optimization was demonstrated in the form of the indentation moduli of each

phase obtained by nanoindentation. Secondly, the SFE of γ , which was evaluated using the single crystal elastic constants and through a peak analysis of the ND data, was correlated with deformed microstructure observed by scanning transmission electron microscopy (STEM).

The material was high-nitrogen DSS with the following composition (in wt.%): 17.2Cr, 5.9Mn, 2.54Mo, 5.01W, 0.43N, 0.012C balance Fe. The alloy was fabricated by means of pressurized induction melting and was homogenized at 1250 °C for 2 h under an argon atmosphere. After hot-rolling into a sheet with a thickness of 4 mm, the sample was solution-treated at 1090 °C for half an hour and water quenched.

In-situ ND experiment was carried out using a residual stress instrument at Korea Atomic Energy Research Institute. A plate type tensile specimen with a total length of 100 mm and a gauge length of 25 mm was installed in a tensile loading machine. Neutron measurements were performed at diffraction angles 2θ of 41.0°, 60.4°, and 76.0° for (110), (200), and (112) diffraction peaks of α , respectively, and 2θ of 47.0°, 83.3°, and 88.0° for (200), (311), and (222) diffraction peaks of γ , respectively. A number of static loading stages were used to measure ND peaks from the specimen loaded with a strain rate of $\sim 4 \times 10^{-4} \text{ s}^{-1}$ under a controlled load of 1 kN in the elastic region, followed by displacement control corresponding to a strain of 0.1. After the ND experiment, thin foil for STEM was prepared in a twin-jet electrolytic polishing apparatus using a solution containing 15% perchloric acid and 85% methanol. The microstructure of the deformed specimen was examined by a scanning transmission electron microscope (JEM2100F, JEOL) at 200 kV.

Another specimen was prepared by mechanical polishing with a diamond suspension followed by electro-polishing with a 10% perchloric

* Corresponding author.

E-mail address: hnhan@snu.ac.kr (H.N. Han).

acid/ethanol solution for nanoindentation. Total 625 indentations on a 25×25 grid of the normal direction plane, $5 \mu\text{m}$ away from each point, were performed at room temperature with Hysitron TriboLab nanoindentation system. A sphere tip with a calibrated radius of curvature of approximately 560 nm was used for all tests at a loading rate of $150 \mu\text{N s}^{-1}$ with a maximum load of $3000 \mu\text{N}$. After the nanoindentation process, EBSD measurements were taken for the crystal phase and orientation mapping of the indented region. The cropped phase and orientation maps are shown in Fig. 1(a) and (b), respectively. Also, EBSD measurements were performed in the normal and rolling direction planes to find the texture development. However, no strong texture was observed in both phases.

From the diffraction peak shift of the ND experiment, the lattice strains of various $\{hkl\}$ planes, ε_{hkl} , for which the plane normals are parallel to the loading direction, were calculated with the following equation:

$$\varepsilon_{hkl} = \frac{d_{hkl} - d_{hkl}^0}{d_{hkl}^0} \quad (1)$$

Here, d_{hkl}^0 and d_{hkl} are the interplanar spacings at the reference and loaded state, respectively. Fig. 2(a) and (b) shows the development of the lattice strains of γ and α , respectively, as the macroscopic applied stress was increased. During the initial loading part, wherein the applied stress is less than $\sim 410 \text{ MPa}$, the lattice strains of both phases increase linearly in the purely elastic region.

To estimate the single crystal elastic constants, C_{ij} , of each phase, the ESC model for polycrystal [12] was adopted. The stress–strain relationship of a specifically oriented grain is described considering the interaction with a uniform sample matrix as follows,

$$\varepsilon^c = (C^{s-1} + U:C^{s-1}) : \sigma^s \quad (2)$$

$$U = -(C^c - C^s + C^s:S^{-1})^{-1} : (C^c - C^s) \quad (3)$$

where \mathbf{C} and \mathbf{S} represent the elastic stiffness tensor and the Eshelby tensor [13] assuming ideal sphere grains in the sample coordinate system, respectively. The superscripts c and s indicate the crystal and the sample, respectively. 5832×2 discrete orientations with volume weights for each phase through division of the Bunge–Euler space $\{\varphi_1, \Phi, \varphi_2\} = \{[0, \pi/2], [0, \pi/2], [0, \pi/2]\}$ into $5 \times 5 \times 5^\circ$ unit boxes were given as the texture input data obtained from EBSD.

The ESC model was combined with an optimization process, where a generic algorithm (GA) [14] in the commercial software MATLAB (R2004a) was utilized. It is well known that the GA is useful for finding the global minimum of an objective function without its derivative in a multi-dimensional problem. The optimized set of variables which

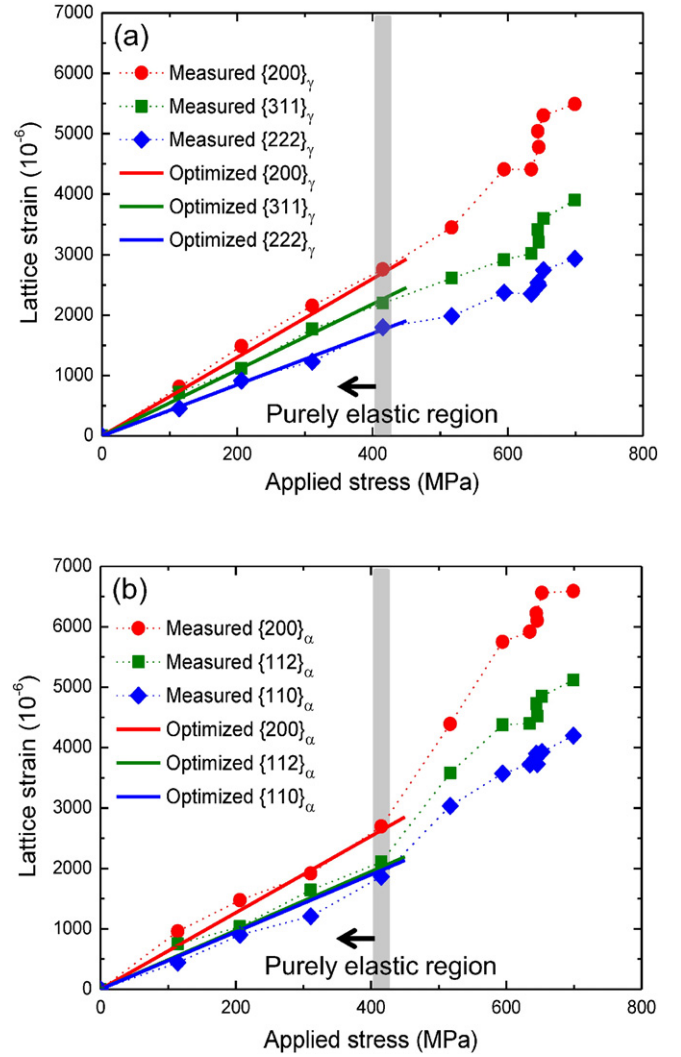


Fig. 2. Evolution of the lattice strains of several $\{hkl\}$ planes of (a) γ and (b) α as a function of the applied stress in the loading direction.

minimizes the differences between the calculated lattice strains and the measured ones from the ND experiment was extracted. The cubic anisotropy ratio $Z = 2C_{44}/(C_{11} - C_{12})$ in the range of $1.5 \sim 3.5$ for both phases was enforced as a constraint. The finally optimized sets of single crystal elastic constants were $(C_{11}^{\gamma}, C_{12}^{\gamma}, C_{44}^{\gamma}, C_{11}^{\alpha}, C_{12}^{\alpha}, C_{44}^{\alpha}) = (206.7, 134.0, 113.5, 221.9, 143.6, 113.8) \text{ GPa}$ and the calculated lattice strains

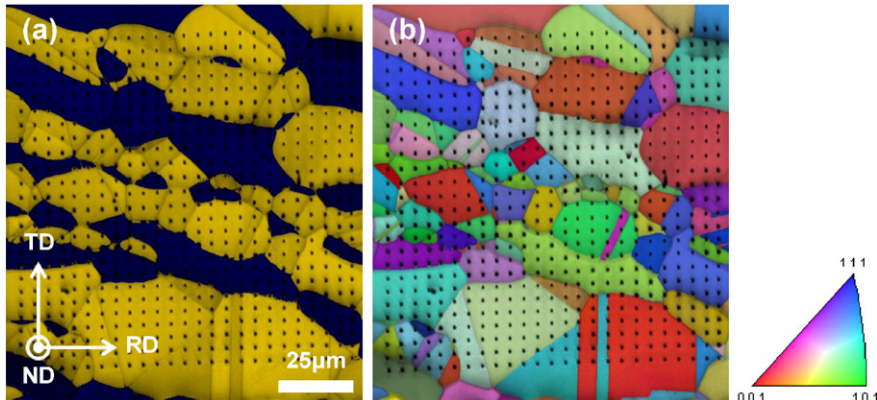


Fig. 1. (a) Phase map (yellow: γ , blue: α) and (b) orientation map of the indented region by EBSD measurement.

Download English Version:

<https://daneshyari.com/en/article/1498047>

Download Persian Version:

<https://daneshyari.com/article/1498047>

[Daneshyari.com](https://daneshyari.com)